Journal of Structural Geology, Vol. 5, No. 3/4, pp. 279 to 286, 1983.
Printed in Great Britain

0191–8141/83 $3.00 + 0.00

Application of the Mohr-circle construction to problems of inhomogeneous deformation

W. D. MEANS

Department of Geological Sciences, State University of New York at Albany, 1400 Washington Avenue, Albany, NY 12222, U.S.A.

(*Received* 17 *June* 1982; *accepted in revised form* 20 *December* 1982)

Abstract—Off-axis Mohr circles are used to represent asymmetric second-order tensor quantities that describe deformation with homogeneous position gradients or flow with homogeneous velocity gradients. The validity of this representation is demonstrated. Several applications to problems of inhomogeneous deformation are explored by considering neighboring domains A and B that are homogeneously but differently deformed or flowing. The compatibility condition in Mohr space is that the circles for A and B should intersect in a point that represents the material line of the A/B boundary. In the first application it is assumed that the stretch tensor is known for each domain, and a Mohr construction is used to find the orientation of a compatible A/B boundary and the rotation of one domain with respect to the other. The second application is similar but involves the instantaneous state of a system. Non-parallel simple shearing at known rates is assumed in A and B, and a construction is used to find the instantaneous orientation of a compatible boundary and the spin of one domain with respect to the other. The third and fourth applications apply Mohr circles to problems of deformation interpolation and deformation averaging. In the former a deformation and shape is found for a domain C that lies between A and B, themselves incompatible, such that the A/C and C/B boundaries are both compatible.

NOMENCLATURE

D	position gradients tensor, forward deformation
d	position gradients tensor, backward deformation
L	velocity gradients tensor
l_{ij}	direction cosines relating sets of orthogonal, Cartesian axes
R	rotation tensor, forward deformation
S	right stretch tensor, forward deformation
S'	left stretch tensor, forward deformation
s'	right stretch tensor, backward deformation
s	left stretch tensor, backward deformation
T	second-order tensor, unspecified
W	vorticity vector
w	vorticity tensor
X_i	coordinates in earlier state, conventional undeformed state
x_i	coordinates in later state, conventional deformed state
$\dot{\gamma}$	engineering shear-strain rate
$\dot{\epsilon}$	strain-rate tensor
θ	counterclockwise rotation of new two-dimensional reference axes relative to old axes
ω	angular velocity magnitude.

INTRODUCTION

MOHR circles centered on the horizontal axis of Mohr diagrams have been used for many years to provide a geometric representation of symmetric second-order tensor quantities, like the state of stress at a point or the state of strain. Recently Robin (1977), De Paor (1979) and Lister & Williams (1983) have employed Mohr circles that are not centered on the horizontal axis of Mohr diagrams, to represent asymmetric second-order tensors, and De Paor (this issue) has found an antique example of the idea in the work of De La Hire (1685). The aims of this paper are to show why Mohr circles provide valid representations of any second-order tensor, symmetric or asymmetric, and to explore some applications that arise in the study of bodies that have been inhomogeneously deformed. The discussion is restricted to two-dimensional cases and to tensors referred to orthogonal Cartesian axes.

MOHR CIRCLES FOR ASYMMETRIC TENSORS

Consider any second-order tensor **T** with components

$$T_{ij} = \begin{bmatrix} T_{11} & T_{12} \\ T_{21} & T_{22} \end{bmatrix}, \tag{1}$$

where T_{12} is different from T_{21} and the tensor is by definition asymmetric. A circle can be constructed in T_{ii}, T_{ij} ($i \neq j$) space for given values of the components as shown in Fig. 1. Points are plotted with coordinates (T_{11}, $-T_{21}$) and (T_{22}, T_{12}). A line is drawn between these points and a circle is drawn about the line as diameter. The circle has its center at (a, b) and diameter D, where

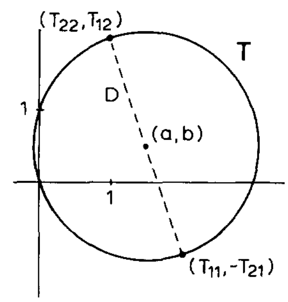

$$T_{ij} = \begin{bmatrix} T_{11} & T_{12} \\ T_{21} & T_{22} \end{bmatrix} = \begin{bmatrix} 2 & 2 \\ 1 & 1 \end{bmatrix}$$

Fig. 1. Mohr circle for an asymmetric second-order tensor **T** with components as given. (a, b) are the coordinates of the center of the circle and D is its diameter.

$$2a = T_{11} + T_{22} \quad (2)$$

$$2b = T_{12} - T_{21} \quad (3)$$

$$D^2 = (T_{12} + T_{21})^2 + (T_{11} - T_{22})^2. \quad (4)$$

This circle turns out to be a Mohr circle representing the tensor **T**. Before demonstrating this we underscore two steps in the construction. We reverse the sign of T_{21} before treating it as a coordinate value in Mohr space, and we use pairs of values in *columns* of matrix (1) to locate each point in Mohr space. The sign change will be familiar to those used to the difference between tensor and Mohr circle sign conventions for stresses or strains. Either T_{12} or T_{21} can be changed. The resulting two Mohr circles are mirror images of each other across the horizontal axis. Here we arbitrarily reverse the sign of T_{21}. Plotting pairs of values from columns rather than rows of (1) is required to ensure that each point on the Mohr diagram represents geometrical attributes of some particular material line, where **T** is an asymmetric tensor involving either deformation or a state of flow.

If the quantities (1) are components of a second-order tensor, then by definition

$$T'_{kl} = l_{ki} l_{lj} T_{ij} \quad (5)$$

where the T'_{kl} are components of the tensor with respect to axes rotated θ degrees counterclockwise from the original axes, and where the l_{ij} for the two dimensional case are

$$l_{ij} = \begin{bmatrix} l_{11} & l_{12} \\ l_{21} & l_{22} \end{bmatrix} = \begin{bmatrix} \cos\theta & \sin\theta \\ -\sin\theta & \cos\theta \end{bmatrix}.$$

This is the transformation formula for any second-order orthogonal Cartesian tensor whether it be symmetric or asymmetric.

To demonstrate that the circle of Fig. 1 is a Mohr circle we have to show that the points $(T'_{11}, -T'_{21})$ and (T'_{22}, T'_{12}) always plot at opposite ends of some diameter of the same circle, no matter how we choose θ. In short, we have to show that the parameters of the circle (a, b and D) are invariant under the transformation (5), or that the quantities on the right-hand side of (2)–(4) are invariant.

By (5)

$$T'_{11} = \cos^2\theta\, T_{11} + \cos\theta\sin\theta\, T_{12} + \sin\theta\cos\theta\, T_{21} + \sin^2\theta\, T_{22} \quad (6)$$

and

$$T'_{22} = \sin^2\theta\, T_{11} - \sin\theta\cos\theta\, T_{12} - \cos\theta\sin\theta\, T_{21} + \cos^2\theta\, T_{22}. \quad (7)$$

Substituting these into (2) yields a primed value of 2a

$$2a' = (\cos^2\theta + \sin^2\theta)\, T_{11} + (\sin^2\theta + \cos^2\theta)\, T_{22} = T_{11} + T_{22}$$

which is evidently always equal to the unprimed value. 2a is therefore invariant. This could have been recognized immediately, since $T_{11} + T_{22}$ is the 'first invariant' or 'trace' of any two-dimensional, second-order tensor.

Again by (5)

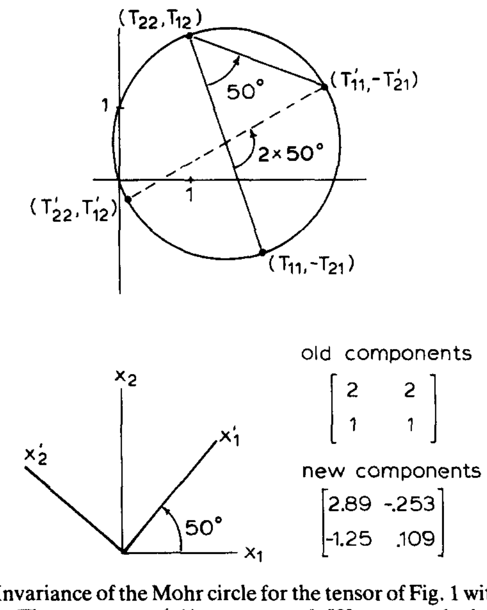

Fig. 2. Invariance of the Mohr circle for the tensor of Fig. 1 with change of axes. The new axes (x'_i) are rotated 50° counterclockwise with respect to the old axes (x_i). The new components of **T** plot on the same circle as the old components.

$$T'_{12} = -\cos\theta\sin\theta\, T_{11} + \cos^2\theta\, T_{12} - \sin^2\theta\, T_{21} + \sin\theta\cos\theta\, T_{22} \quad (8)$$

$$T'_{21} = -\sin\theta\cos\theta\, T_{11} - \sin^2\theta\, T_{12} + \cos^2\theta\, T_{21} + \cos\theta\sin\theta\, T_{22}. \quad (9)$$

Substituting these into (3) yields

$$2b' = (\cos^2\theta + \sin^2\theta)\, T_{12} - (\sin^2\theta + \cos^2\theta)\, T_{21} = T_{12} - T_{21},$$

so 2b is also invariant.

Substituting (6)–(9) into (4) and combining some terms we obtain

$$D^2 = [-2(\cos\theta\sin\theta)(T_{11} - T_{22}) + (\cos^2\theta - \sin^2\theta) \times (T_{12} + T_{21})]^2 + [(\cos^2\theta - \sin^2\theta)(T_{11} - T_{22}) + 2(\cos\theta\sin\theta)(T_{12} + T_{21})]^2.$$

Squaring and combining like terms, this becomes

$$D^2 = [(\cos^2\theta - \sin^2\theta) + (2\cos\theta\sin\theta)^2] \times [(T_{11} - T_{22})^2 + (T_{12} + T_{21})^2]$$

which equals $(T_{11} - T_{22})^2 + (T_{12} + T_{21})^2$ since the quantity in the first brackets is alway equal to 1. Therefore D^2, like 2a and 2b, is invariant under (5), and the circle of Fig. 1 is a Mohr circle in the sense that the components of a given tensor **T** always plot on it no matter how the axes are chosen. Figure 2 shows an example of this invariance of the circle with changes of axes. The points $(T_{11}, -T_{21})$ and (T_{22}, T_{12}) define the diameter of the circle with respect to the original axes, as in Fig. 1. The points $(T'_{11}, -T'_{21})$ and (T'_{22}, T'_{12}) define another diameter of the same circle when the axes are rotated 50 degrees counterclockwise. Note that the angle and sense of rotation of the new axes with respect to the old axes corresponds to half the rotation required to bring the diameter connecting the old components on the Mohr circle into coincidence with the diameter connecting the corresponding new components.

Mohr circles for the velocity gradients tensor and the position gradients tensor

The components of these asymmetric tensors are respectively the coefficients L_{ij} in the velocity equations

$$\begin{aligned} v_1 &= L_{11}x_1 + L_{12}x_2 \\ v_2 &= L_{21}x_1 + L_{22}x_2 \end{aligned} \tag{10}$$

and the coefficients D_{ij} in the coordinate transformations

$$\begin{aligned} x_1 &= D_{11}X_1 + D_{12}X_2 \\ x_2 &= D_{21}X_1 + D_{22}X_2. \end{aligned}$$

Equations (10) give the instantaneous velocity components (v_1, v_2) at any position (x_1, x_2) in space. Where the L_{ij} are numbers themselves independent of position, the equations describe a velocity field with homogeneous velocity gradients and, accordingly, with identical strain-rate and vorticity at every point. Equations (11) give the deformed coordinates of any particle (x_1, x_2) in terms of its undeformed coordinates (X_1, X_2). Where the D_{ij} are independent of position in space, the equations describe a homogeneous deformation with identical strain and rotation at every point. The quantities D_{ij} are commonly but misleadingly called 'deformation gradients' (e.g. Truesdell & Toupin 1960, p. 245, Malvern 1969, p. 156, Means 1976, p. 173 and 1982, p. T2). Here such quantities are called *position gradients*, following Segel (1977, p. 184). The tensor **D** is called the *position gradients tensor*. The term deformation gradients tensor is reserved for third-order tensors which describe how the D_{ij} or the d_{ij} (see later) vary with position.

Figures 3(a) and (b) show heavy circles representing the tensors **L** and **D**. Each can be thought of as containing a symmetric part relating to strain and an asymmetric part relating to rotation. For the velocity gradients tensor **L**, the two parts are combined additively. The decomposition of **L** into these two parts is represented in Mohr space by moving the circle vertically until it is centered on the horizontal axis (Lister & Williams 1982). In this position, the circle represents the symmetrical strain-rate component $\dot{\epsilon}$ of **L**. The vertical displacement represents the antisymmetrical vorticity component **w** of **L**. The vertical displacement in Mohr space is $W/2$, where W is the magnitude of the vorticity vector (see Means *et al.* 1980).

The tensor **D** is differently decomposed into symmetric and asymmetric parts. Here the two are combined multiplicatively, and their *polar* decomposition is represented in Mohr space by swinging the **D** circle on a circular arc about the origin until it is centered on the horizontal axis. The circle there represents the symmetric right stretch tensor **S** of **D** (see Malvern 1969, p. 173), while the angle of rotation represents the rotation **R**. Notice that for both decompositions the diameters of the circles for the total asymmetric tensors are equal to the diameters for their symmetric parts.

The Cartesian coordinates of points on any **L** or $\dot{\epsilon}$ circle represent the longitudinal strain-rate $\dot{\epsilon}$ and angular velocity ω of particular material lines (Lister & Williams 1982). The axes of this type of Mohr diagram can

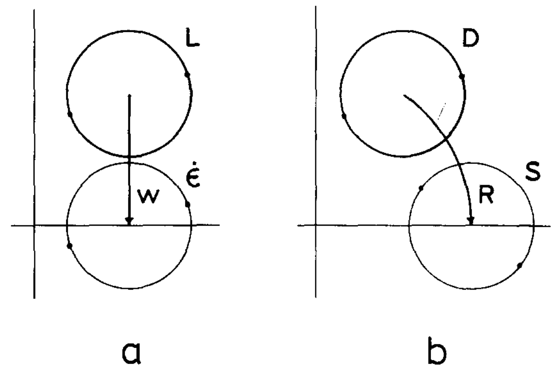

Fig. 3. Decomposition of the tensors **L** and **D** into symmetric and asymmetric components. (a) Decomposition of **L** into its vorticity and strain-rate components. (b) Decomposition of **D** into its rotation and right stretch components. In both diagrams the points on the circle represent material lines parallel to the axes of reference.

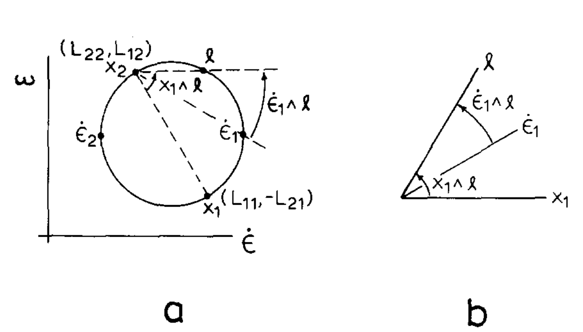

Fig. 4. Mohr circle for a velocity gradients tensor (a) and corresponding diagram in geographic space (b). Points on the circle with maximum and minimum $\dot{\epsilon}$ coordinates represent material lines in the principal directions of the strain-rate tensor. A general point l on the circle represents a material line inclined as shown in (b) to the x_1 and $\dot{\epsilon}_1$ directions.

accordingly be labelled $\dot{\epsilon}$ and ω as in Fig. 4. For the special case of zero vorticity, and for this case only, the vertical coordinate can also be interpreted as the tensor shear-strain rate $\dot{\gamma}/2$. For all other cases the vertical coordinate is the angular velocity of a material line with respect to the coordinate axes.

The orientation of the material line l represented by any point l on an **L** or $\dot{\epsilon}$ circle is read as shown in Fig. 4. The angles $x_1 \wedge l$ or $\dot{\epsilon}_1 \wedge l$ measured in the Mohr diagram are equal in magnitude and sense to the corresponding angles in geographic space (Fig. 4b).

Since L_{11} and $-L_{21}$ are the extension rate and angular velocity of the material line instantaneously under (parallel to) the x_1 axis, we can refer to the (L_{11}, $-L_{21}$) point on the **L** circle as the x_1 point. Similarly the (L_{22}, L_{12}) point is the x_2 point. This simpler annotation on the Mohr diagrams will be used in what follows, for **D** and **S** as well as for **L** and $\dot{\epsilon}$ circles.

The Cartesian coordinates of points on **D** or **S** circles have no simple significance in terms of longitudinal strains and rotations of material lines, but the *polar coordinates* about the origin of the graph do have simple significance (Means 1982). The radial coordinate of any point on a **D** or **S** circle is the stretch of a material line. The angular coordinate is the rotation of the same material line. The stretch is read using the scale laid out along the Mohr axes; the rotation is read by measuring

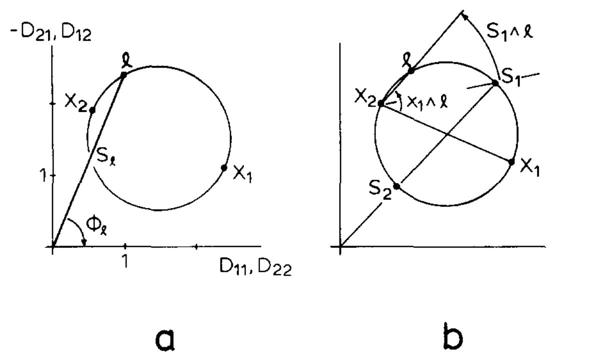

Fig. 5. Mohr circle for a position gradients tensor. (a) Points X_1 and X_2 [at $(D_{11}, -D_{21})$ and (D_{22}, D_{12}), respectively] represent material lines parallel to the axes of reference in the undeformed state. A general point l represents a material line with stretch S_l and rotation ϕ_l is given by its polar coordinates (in this case 2.6 and 67° clockwise). (b) Same circle, showing how to read the orientation of l with respect to X_1 in the undeformed state and with respect to the principal stretch direction S_1. Points S_1 and S_2 on the circle at maximum and minimum distances from the origin represent material lines parallel to the principal directions of the right stretch tensor.

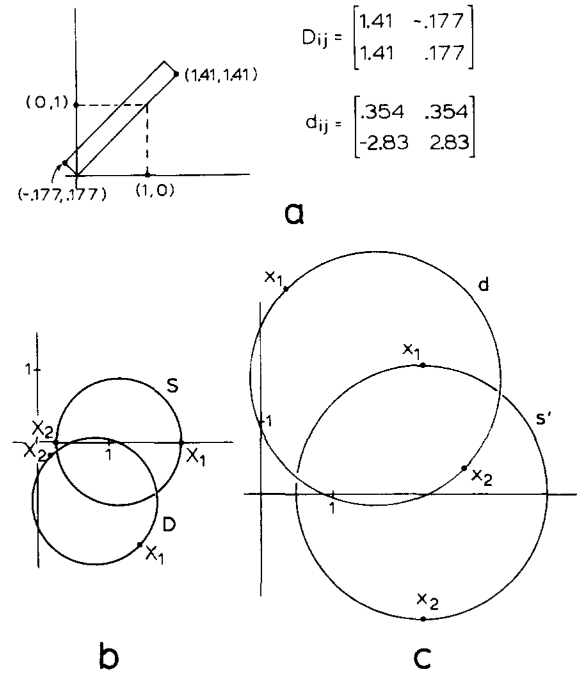

Fig. 6. Mohr circles for a deformation with rotation and area change. (a) The deformation in geographic space. The components of **D** can be read from the deformed coordinates of particles initially at (1, 0) and (0, 1), which become (D_{11}, D_{21}) and (D_{12}, D_{22}), respectively; d_{ij} are position gradients for the backwards deformation that would convert the rectangle back into the square. (b) Mohr circles for **D** and its right stretch tensor **S**. (c) Mohr circles for **d** and its right stretch tensor **s**′.

the angle from the ray to a point *toward the horizontal axis* of the diagram (Fig. 5a). These relations are demonstrated in Means (1982) for the **S** circle. They also apply to the **D** circle, since the rotation of any line is the sum of the rotation due to strain and the extra rotation imposed on all lines by the (rigid body) rotational component of **D**.

The material line represented by any point on a **D** or **S** circle is found by measuring the angles $X_1 \wedge l$ or $S_1 \wedge l$ as shown in Fig. 5(b). Note that these are angles measured in the *undeformed state*.

Mohr circle for the reciprocal position gradients tensor

Equations (11) gave the deformed coordinates in terms of the undeformed coordinates. Inversion gives equations

$$X_1 = D^{-1}{}_{11}x_1 + D^{-1}{}_{12}x_2$$
$$X_2 = D^{-1}{}_{21}x_1 + D^{-1}{}_{22}x_2 \qquad (11)$$

which represent the imaginary backward deformation that would convert the deformed coordinates of particles back into the undeformed coordinates. The components of $\mathbf{D}^{-1}$, the reciprocal position gradients tensor, also designated **d**, are related to the components of **D** for the forward deformation by

$$d_{ij} = \begin{bmatrix} d_{11} & d_{12} \\ d_{21} & d_{22} \end{bmatrix} = \begin{bmatrix} D_{22}/\Delta & -D_{12}/\Delta \\ -D_{21}/\Delta & D_{11}/\Delta \end{bmatrix},$$

where

$$\Delta = (D_{11}D_{22} - D_{12}D_{21}).$$

A Mohr circle can be drawn for **d** just as for **D** and the decomposition is also similar. Now the symmetric component, represented by the circle when it is swung until centered on the horizontal axis, is the right stretch tensor of the backward deformation **s**′, or the inverse of the left stretch tensor of the forward deformation **S**′. Similarly, the left stretch tensor of the backward deformation **s** is the inverse of the right stretch tensor of the forward deformation **S**,

$$\mathbf{s}' = \mathbf{S}'^{-1}$$
$$\mathbf{s} = \mathbf{S}^{-1}.$$

Mohr circles for **d** and **s**′ involve angles measured in the deformed state. Figure 6 shows a rotational deformation with area change and the corresponding Mohr circles for **D**, **S**, **d** and **s**′.

APPLICATION TO PROBLEMS OF INHOMOGENEOUS DEFORMATION

Consider the simple situation in which an inhomogeneously deformed region is made up of two kinds of homogeneously deformed domains, A and B, that adjoin one another across boundaries of zero width. For compatibility of deformation across such a boundary, lines parallel to the boundary in domains A and B must be identically stretched or shortened and identically rotated in some common frame. The equivalent requirement in Mohr space is that the circles for **D** or **L** in domains A and B must intersect in a point that represents the line of the boundary on both circles (Fig. 7a). Where the circles fail to intersect, or intersect in points representing different orientations of lines on the two circles, the compatibility condition is not satisfied (Fig. 7b).

Circles that intersect at two points prompt the question: can *two* orientations of lines simultaneously satisfy the compatibility requirements? Can there be 'checker-

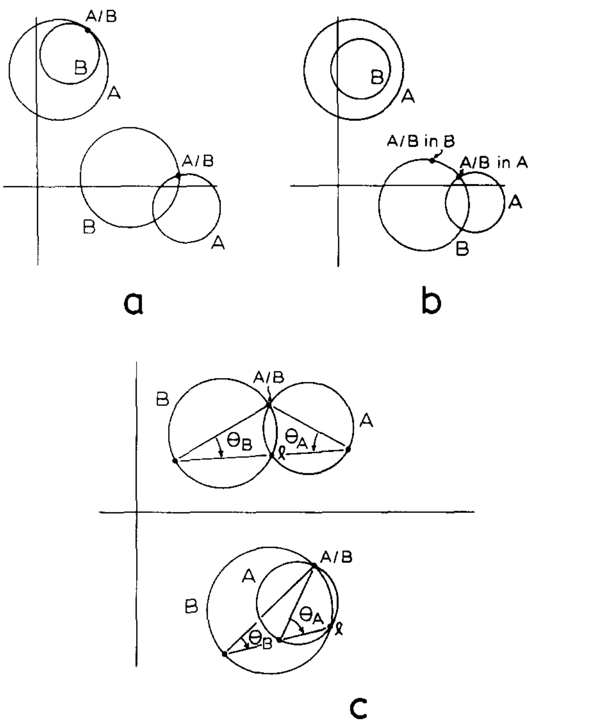

Fig. 7. Pairs of Mohr circles representing homogeneous but different deformations in adjacent domains A and B. In (a) the circles intersect in a point representing the line of a compatible boundary A/B between the two domains in geographic space. In (b) the circles fail to intersect, or intersect in a point representing differently oriented lines in the two domains, so the boundary A/B is not a compatible boundary. (c) shows why there can never be more than one orientation of compatible boundary between two homogeneously deformed domains. A/B is assumed to be one compatible boundary and the other point of intersection l represents a candidate for a second compatible boundary. For the top case the inclinations of $l(\theta)$ to the first boundary A/B are always different in *sense* in the two domains. In the bottom case they are always different in *magnitude*. Hence l can never be a second compatible boundary.

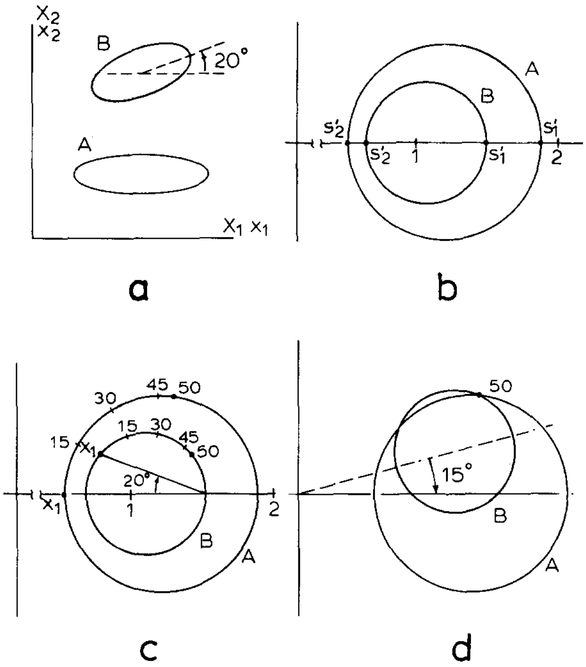

Fig. 8. Mohr-circle solution to the problem of finding relative rotation of two compatible domains when their strains are known. (a) Ellipses representing states of strain in domains A and B. (b) Mohr circles for the right stretch tensor of the backwards deformations s′ in each domain. s'_1 and s'_2 are the principal stretches of the backwards deformation. (c) Same circles showing positions of points representing material lines in the deformed state in the x_1 axial direction and at various angles, measured clockwise, from the x_1 direction. (d) Rotation of the circle for domain B to bring a calibration mark (the 50° mark) on circle B into coincidence with the same mark on circle A.

board' deformation fields? Figure 7(c) shows that this is never possible. Compatible arrays of A and B must involve only one orientation of compatible boundary, as in the 'banded deformation structures' of Cobbold (1977). By the same argument, individual A/B boundaries must always be straight, never curved, so long as A and B are homogeneously deformed. The foregoing general observations apply equally to two-domain finite deformations and to two-domain infinitesimal deformation or rate-of-deformation fields. We now turn to more specific problems.

Determination of relative rotation of two domains from knowledge of their finite strains

In general, if domains A and B are differently strained from one another, yet deformed compatibly across their mutual boundary, the difference in strains will be accompanied by a difference in rotations, or in other words a rotation of one domain with respect to the other. This can be illustrated with Mohr circles.

Figure 8(a) represents two neighboring exposures, for example in two contrasted lithologies, in which the state of strain is different. We assume that the strain field is homogeneous within each lithology and that the two lithologies adjoin across a sharp contact. We ask how the observed states of strain in A and B may be used to establish the existence and orientation of a compatible A/B boundary and how domain B must have rotated with respect to domain A.

Identical reference axes for the deformed and undeformed states are selected parallel to the principal directions of strain in domain A (Fig. 8a). This renders the rotation of A zero and any rotation of B is thus the rotation of B with respect to A. The components of S′ are then written for domain A,

$$S'_{\mathrm{Aij}} = \begin{bmatrix} 1.88 & 0 \\ 0 & 0.53 \end{bmatrix}, \qquad (12)$$

and for domain B in axes parallel to its own deformed principal directions

$$S'_{\mathrm{Bij}} = \begin{bmatrix} 1.45 & 0 \\ 0 & 0.69 \end{bmatrix}. \qquad (13)$$

This is the left stretch tensor for the forward deformation in domain B, or in other words the strain in B, if it is thought of as following the rotational part of the forward deformation of B. For domain A, S′ is indistinguishable from S since there is no rotation of A. Next each of these matrices is inverted to yield components of the respective right stretch tensors s′ of the backwards deformation.

$$s'_A = \begin{bmatrix} 0.53 & 0 \\ 0 & 1.88 \end{bmatrix}$$

$$s'_B = \begin{bmatrix} 0.69 & 0 \\ 0 & 1.45 \end{bmatrix}. \quad (14)$$

Components (14) represent the unstraining of B without rotation of its principal directions from their deformed orientation, in a local reference frame still parallel to the principal directions in B.

The Mohr circle for s'_A is drawn, and this also represents $\mathbf{d}_A$ since we have eliminated any rotation of A by choice of axes. The circle for s'_B is then drawn and is seen not to intersect the circle for A (Fig. 8b). There is evidently no possibility of a compatible A/B boundary unless we add a rotation to B. This is represented by swinging the B circle about the origin until it intersects the A circle in a point representing the same material line on both circles. To find the direction and amount of the requisite rotation, we identify points on each circle representing lines parallel to the x_1 and x_2 axes, and lines in various orientations measured clockwise from the x_1 axis. For circle A, the x_1 and x_2 points are coincident with the s'_2 and s'_1 points, respectively. In domain B, x_1 is inclined 20° clockwise from the s'_2 $(= S'_1)$ direction. The x_1 point on circle B can accordingly be found by drawing a chord from the right-hand extremity of the circle that is inclined 20° clockwise from the horizontal axis (Fig. 8c).

Once both circles are calibrated, some arcs are swung about the origin until one is found that connects calibration marks bearing the same number. For the present case, such an arc is the one connecting points representing lines 50° clockwise from x_1. This is the orientation in the deformed state of a compatible A/B boundary. Its backward stretch can be read as 1.46, so the forward stretch is 0.68. The rotation of B is given by the angle through which the B circle must be swung to return from the position shown in Fig. 8(d) to the position shown in Fig. 8(b). In this case it is 15° clockwise for the backward deformation represented by the Mohr diagram, or 15° counterclockwise for the forward deformation.

Determination of the relative spin of two domains from their strain-rates

This is an analogous problem to the preceding one, but involves instantaneous deformation rates rather than finite deformations, and a correspondingly simpler Mohr construction. Imagine adjacent domains A and B, perhaps single crystals, that are undergoing dextral simple shearing at the same rate but in different directions (Fig. 9a). We ask if there is a boundary across which the two deformations are instantaneously compatible, and if so, what is the necessary angular velocity or spin of the shear planes in B with respect to the shear planes in A?

Axes are chosen with x_1 parallel to the shear direction in A. A calibrated Mohr circle for **L** in A is drawn as in Fig. 9(b). It is a circle centered on the ω axis with its x_1 point at the origin, since lines parallel to x_1 in A have zero longitudinal strain-rate and zero angular velocity.

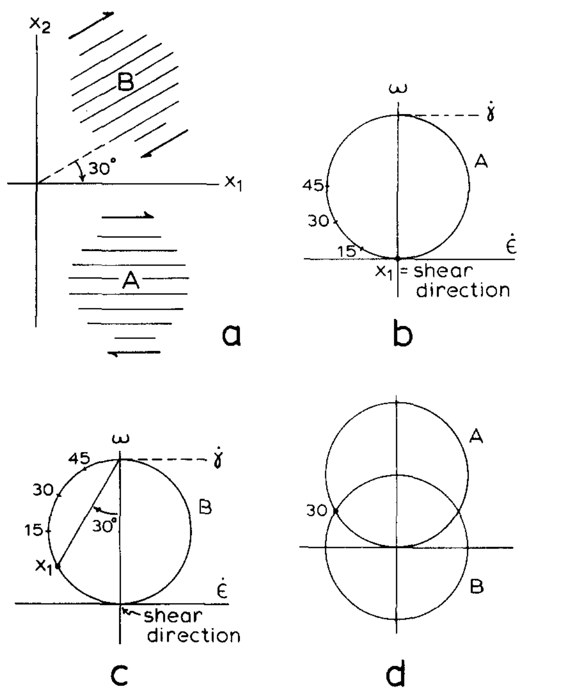

Fig. 9. Mohr-circle solution to the problem of finding relative spin of two compatible domains when their strain-rates are known. (a) Adjacent simple shearing domains A and B. (b) Calibrated Mohr circle for L in domain A. (c) Calibrated Mohr circle for L in domain B, assuming initially that the shear planes are not spinning with respect to the reference axes. (d) Same circles as in parts (b) and (c) but with the circle for B displaced vertically to bring the 30° calibration marks into coincidence on the two circles. This displacement in Mohr space corresponds in geographic space to adding a counterclockwise spin to the shear planes in B, to achieve instantaneous compatibility with A. (An alternative solution in this case is to spin B at the same rate clockwise, to achieve compatibility across a boundary 120° clockwise from x_1).

The x_2 point on the circle is diametrically opposite, at (0, $\dot{\gamma}$). Various other points are identified by the angle that the corresponding lines make with the x_1 direction.

Next a calibrated circle is drawn for **L** in B assuming for the moment that B like A has its shearing planes fixed in the designated reference frame. This circle is shown in Fig. 9(c). It is identical in size and position to the circle for A but all the calibration marks are rotated 60° clockwise because the x_1 axis is inclined 30° clockwise from the shear planes in B. If the circles of Figs. 9 (b) & (c) are imagined superposed, it is clear that no common point on the circles will bear the same calibration number. There is accordingly no possible compatible boundary between domains A and B until we relax the assumption made above that the shear planes in B are not rotating. Relaxing this requirements means in Mohr space that we are free to move the B circle vertically up or down to see if this brings about any coincidence of the same calibration marks. It does for the 30° clockwise mark (Fig. 9d). This signifies that a boundary inclined 30° clockwise from x_1 is an instantaneously compatible boundary between the two domains. It is shortening at a longitudinal strain rate of 0.43 $\dot{\gamma}$ and rotating clockwise 0.25 $\dot{\gamma}$. The extra angular velocity that had to be imposed on B to bring compatibility about is represented by the vertical distance through which the B circle had to be moved from Fig. 9(c) to Fig. 9(d). It is 0.5 $\dot{\gamma}$ and corresponds to a counterclockwise spin of the shear planes in B relative to those in A. Notice the interesting result in this case that to make the instantaneous deformation compatible in two simple shearing domains, we have converted the deformation in one of them into a pure shearing (the **L** circle for B is centered on the origin in Fig. 9d).

Interpolation of deformation in a domain between two incompatible domains

In the preceding examples, we adjusted the deformation in domain B to make it compatible with the deformation in domain A. This corresponds to physical situations where the deformation in A is independently controlled and B accommodates to it. In other situations, the deformation in B may also be independent so that any incompatibility between A and B has to be accommodated by the appearance of a linking zone C situated between A and B. The deformations in C must often be inhomogeneous, but here we assume the geometrically simple situation in which the deformation in C, like that in A and B, is homogeneous.

Figure 10(a) shows two incompatible deformations in domains A and B. A has undergone simple shear parallel to the x_1 axis while B has undergone pure shear with its S_1 direction parallel to x_1. In the absence of an accommodation zone between these domains there must be slip on the boundary as shown.

Figure 10(b) shows Mohr circles for $\mathbf{D}_A$ and $\mathbf{D}_B$. The shape of an accommodation domain C and the deformation in C are to some extent interdependent. Here we pick orientations for the A/C and B/C boundaries and find the unique deformation in C that makes these compatible boundaries. A/C is picked parallel to the X_1 axis in the undeformed state and B/C is picked rotated 15° counterclockwise from X_1 in the undeformed state. These two points are located on the circles for A and B. The C circle must pass through these points, and thus its center is on the perpendicular bisector (dashed) of this chord of the circle. The center of the C circle is then found by locating that point on the dashed line from which rays to A/C and B/C make an angle twice the angle measured from A/C to B/C in geographic space. In this case the double angle is 30° counterclockwise.

The X_2 point on the C circle can now be plotted diametrically opposite the X_1 point (the point A/C in Fig. 10b) and the coordinates read to give the following description of $\mathbf{D}_C$:

$$D_{Cij} = \begin{bmatrix} 1.0 & 0.39 \\ 0 & 0.70 \end{bmatrix}.$$

These values can in turn be used to draw pictures of the deformation of domain C as in Fig. 10(c). From the geometry of Fig. 10(b), it can be seen how, if zone C is made more parallel-sided, the necessary deformation in C becomes larger.

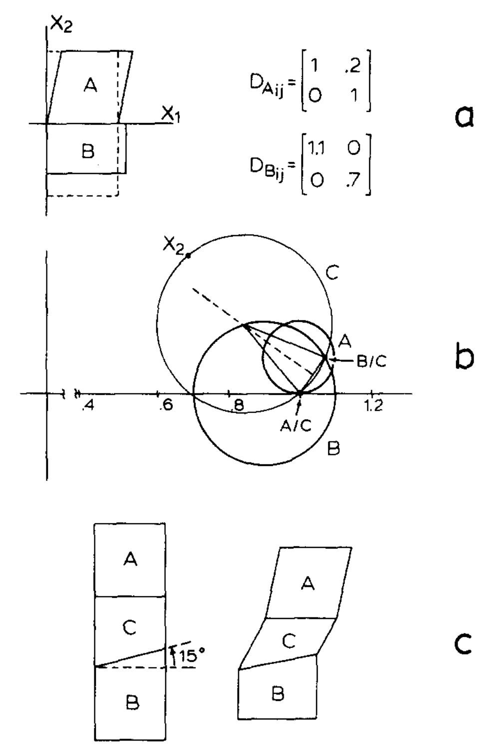

Fig. 10. Mohr-circle solution to the problem of finding the deformation in an accommodation zone C between two incompatibly deformed domains A and B. (a) Incompatible deformations in domains A and B and corresponding components of **D**. (b) Mohr circles for **D** in domains A and B and the construction used to find the circle for zone C as described in text. (c) Deformed and undeformed configurations of domains A, B and C.

Deformation averaging

Deformation averaging, or strain averaging (from field data), is usually undertaken to obtain bulk deformations or bulk strains from information on local deformations or strains within some larger region. Figure 11 shows an example of deformation averaging. The deformations in two domains of equal undeformed area are known. B is sheared parallel to x_1 and flattened perpendicular to x_1. A is flattened perpendicular to x_1 without shear. As Cobbold (1977) has shown, components for the bulk deformation are obtained by weighted averaging of the components of the two domains, component by component. In the example of Fig. 11, A and B are weighted equally because they have equal undeformed areas.

The corresponding Mohr construction is shown in Fig. 11(b). Circles for A and B are drawn with their X_1 and X_2 points identified. Lines are drawn connecting the two X_1's (in this case coincident) and the two X_2's. Each such line is then divided according to the relative weights given A and B, to find the X_1 and X_2 points on the circle for the bulk deformation and hence the circle itself.

Figure 11(c) shows the circles for $\mathbf{D}_A$ and $\mathbf{D}_B$ swung down to positions where they represent $\mathbf{S}_A$ and $\mathbf{S}_B$, the pure strain components of the deformations. It can be seen that the true bulk principal stretch S_1 is intermediate between, but not the average of, S_{A1} and S_{B1}. S_2 for the bulk deformation is not intermediate between S_{A2} and S_{B2} but is greater than both.

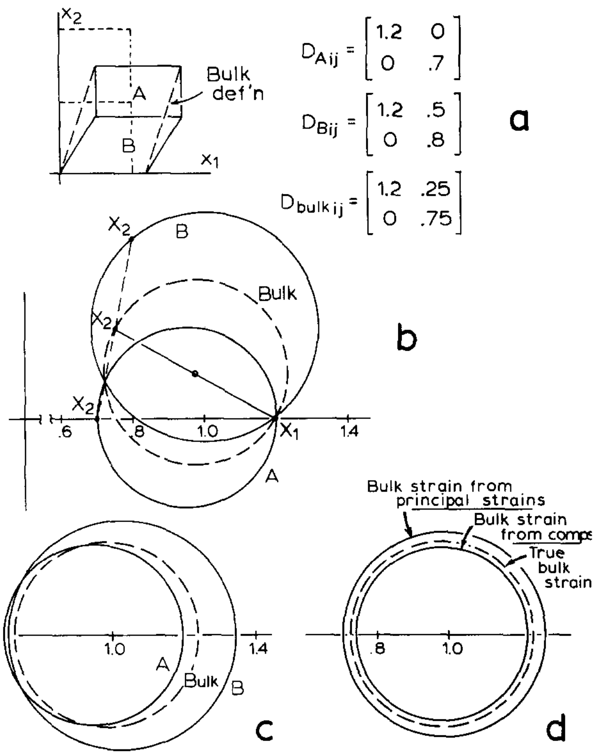

Fig. 11. Mohr-circle constructions for deformation averaging to obtain bulk deformations or bulk strains. (a) Compatible deformations in domains A and B, the corresponding bulk deformation, and components of **D**. (b) Mohr circles for **D** in domains A, B and the construction used to find the circle for the bulk deformation (dashed). (c) Mohr circles for **S** obtained from part (b) by swinging the **D** circles about the origin until they are centered on the horizontal axis. (d) Comparison of the **S** circle representing the true bulk strain (dashed) with the **S** circles corresponding to Oertel's (1981) two methods of strain averaging.

Figure 11(d) compares the Mohr circles for the true bulk strain with the Mohr circles that can be drawn using Oertel's (1981) two strain-averaging techniques. In accordance with Oertel's statements, the circle drawn by averaging the principal strains overestimates the true bulk strain, while the circle drawn by averaging the components in a common frame (averaging the coordinates of the X_1 and X_2 points) underestimates the true bulk strain. The common frame here is the frame of the X axes in the undeformed state, whereas Oertel uses a common frame in the deformed state. The techniques described here can also be used to reproduce this case and to see whether Oertel's generalization holds in other examples.

CONCLUSIONS

Mohr-circle manipulations of the kinds illustrated here may aid in understanding the complex geometry that characterizes even the simplest inhomogeneous deformations. They may also provide a basis for derivation of equations dealing with the same phenomena, or a means of checking the results of using such equations.

Acknowledgements—I thank Peter Cobbold, Jonathan Cutler, Declan De Paor, David Durney, Subir Ghosh, Richard Lisle, Gordon Lister, and Gerhard Oertel for suggesting improvements on the submitted version of the paper. I am particularly indebted to Gordon Lister and Paul Williams for showing me their 1982 paper, which introduced me to the idea of off-axis Mohr circles.

REFERENCES

Cobbold, P. R. 1977. Description and origin of banded deformation structures. I. Regional strain, local perturbations, and deformation bands. *Can. J. Earth Sci.* **14**, 1721–1731.

De La Hire, P. H. 1685. Sectiones Conicae in Novem Libros Distributae, . . . Stephanum Michallet, Parisiis.

De Paor, D. 1979. Stereographic projection of vectors. Programme and Abstracts. Tectonic Studies Group Annual Meeting, University of Nottingham, 18–19 Dec. 1979.

Lister, G. S. & Williams, P. F. 1983. The partitioning of deformation in flowing rock masses. *Tectonophysics* **92**, 1–34.

Malvern, L. E. 1969. *Introduction to the Mechanics of a Continuous Medium*. Prentice-Hall, Englewood Cliffs, New Jersey.

Means, W. D. 1982. An unfamiliar Mohr circle construction for finite strain. *Tectonophysics* **89**, T1–T6.

Means, W. D., Hobbs, B. E., Lister, G. S. & Williams, P. F. 1980. Vorticity and non-coaxiality in progressive deformations. *J. Struct. Geol.* **2**, 371–378.

Oertel, G. 1981. Strain estimation from scattered observations in an inhomogeneously deformed domain of rocks. *Tectonophysics* **77**, 133–170.

Robin, P. F. 1977. Angular relationships between host and exsolution lamellae and the use of the Mohr circle. *Am. Miner.* **62**, 127–131.

Segel, L. A. 1977. *Mathematics Applied to Continuum Mechanics*. Macmillan, New York.

Truesdell, C. and Toupin, R. 1960. The classical field theories. *Encyclopedia of Physics* (S. Flügge, ed.), Springer, Berlin, Vol. 3, 226–793.